Contents lists available at ScienceDirect

Biochemical Pharmacology

Benzylidenemalononitrile compounds as activators of cell resistance to oxidative stress and modulators of multiple signaling pathways. A structure–activity relationship study

Kyril Turpaev [a,b,c,*], Mikhail Ermolenko [a], Thierry Cresteil [a], Jean Claude Drapier [a,**]

[a] Institut de Chimie des Substances Naturelles, UPR2301 CNRS, Centre de Recherche de Gif, 91190 Gif-sur-Yvette, France
[b] Vavilov Institute of General Genetics, Russian Academy of Sciences, 119991 Moscow, Russia
[c] Center for Theoretical Problems of Physicochemical Pharmacology, Russian Academy of Sciences, 119991 Moscow, Russia

ARTICLE INFO

ABSTRACT

Benzylidenemalononitrile (BMN) tyrphostins are well known as potent tyrosine kinase inhibitors. Moreover, in recent years it has been recognized that members of the tyrphostin family possess additional biological activities independent of their ability to inhibit protein tyrosine kinases. In this study, we examined the relationship between the structure of 49 BMNs and related compounds, and their capacity to induce heme oxygenase 1 (HO-1) gene expression in U937 human monocytic cells, to activate upstream signaling pathways and to protect cells against menadione-induced oxidative stress. It was found that the electron-withdrawing (NO_2, CN, halogen) groups in BMN molecules and double meta-MeO substituents increased the HO-1 gene induction, while the electron-donating groups in ortho/para position (OH, MeO and N-morpholino) significantly decreased it. The magnitude of activation of c-Jun, Nrf2, p38 MAPK, and p70S6K correlated with specific substitution patterns in the BMN structure. BMN-dependent maximal up-regulation of HO-1 required parallel increase in Nrf2 and phospho-c-Jun cellular levels. Liquid chromatography mass spectrometry (LC–MS) analysis revealed that BMNs can generate conjugates with one or two glutathione equivalent(s). This study supports the hypothesis that BMNs induce the expression of protective genes by alkylating sensitive cysteine residues of regulatory factors.

1. Introduction

Pharmacological effects of benzylidenemalononitrile (BMN) compounds have been examined since the 1990s when several of their derivatives, referred to as tyrphostins, were recognized as specific inhibitors of epidermal growth factor tyrosine kinase [1,2]. Subsequent design and testing of a series of BMNs revealed new specific inhibitors of various protein tyrosine kinases [2]. Later, it was revealed that BMN tyrphostins possess biological activities unrelated to inhibition of protein kinase activity. For instance, phenolic tyrphostins are antioxidants, free radical scavengers, and mitochondrial uncouplers [3,4]. AG-126-like tyrphostins stimulate

increase in cellular glutathione (GSH) level, inhibit expression of pro-inflammatory genes as iNOS and COX-2, and suppress TNFα release and activation of poly (ADP-ribose) polymerase [3,5]. These tyrphostin-driven effects have been observed in experiments aimed at pharmacological suppression of septic shock, ischemia, inflammation, and injuries caused by radiation and chemotherapy [6–10]. The exact molecular mechanisms mediating the protective effects of BMN compounds remain unclear, but we have previously shown that AG-126 and several other structurally related tyrphostins are potent activators of the expression of heme oxygenase 1 (HO-1), H-ferritin, interleukin 8 (IL-8), and several other, mainly redox-sensitive, genes. Our study also provided evidence that the gene induction capacity of BMN tyrphostins was not related to inhibition of protein tyrosine kinases. We showed that AG-126-like tyrphostins stimulate key regulators of redox-sensitive signaling systems like MAP kinases as well as AP-1 and Nrf2 transcription factors [11]. It is worth noting that BMN compounds have distant structural similarity with curcumin and chalcones. These well-known activators of protective genes have promising anti-inflammatory properties and capacities for preventing tumorigenesis and suppressing angiogenesis [12,13].

The present study was focused on the structure–activity relationship of a wide series of synthetic BMN compounds and

* Corresponding author. Present address: Department of Medical Cell Biology, Uppsala University, Biomedical Center, 75123 Uppsala, Sweden.
Tel.: +46 73 742 53 23; fax: +46 18 471 40 59.
** Corresponding author. Tel.: +46 73 742 53 23; fax: +46 18 471 40 59.
E-mail addresses: kyril.turpaev@yahoo.com (K. Turpaev),
jean-claude.drapier@icsn.cnrs-gif.fr (J.C. Drapier).

related compounds in a human monocytic cell line. BMN biological effects were characterized by measuring HO-1 expression, the activity of upstream signaling systems, and modulation of cell resistance to oxidative stress. Moreover, we have determined the structure of the products generated by reaction between BMNs and GSH, a key component of cellular thiol redox homeostasis.

2. Materials and methods

2.1. Reagents

Tyrphostins AG-9 (4-methoxybenzylidene)malononitrile), AG-10 (4-hydroxy-benzylidenemalononitrile), and AG-126 (3-hy-droxy-4-nitrobenzylidenemalononitrile) were purchased from Calbiochem (San Diego, CA). Chemicals were dissolved in DMSO. In all experiments with cell cultures, the final DMSO concentration in the medium did not exceed 0.05%.

2.2. General procedure for the synthesis of BMN compounds

Most of the BMN compounds were conveniently prepared in high yield by straightforward Knoevenagel condensation of the relevant aldehyde with malononitrile (1.2 equiv.) catalyzed by imidazole (0.01 equiv.) at room temperature in methanol. The products obtained were of at least 98% purity after re-crystallization of the product from methanol, ethanol or heptane. EMK 201 and EMK 211 were prepared from EMK 171 and EMK 181, respectively, by treatment with BBr$_3$ (4 equiv., $-40\,^\circ$C to room temperature). EMK 311 and EMK 321 were prepared by condensation of 3-nitroben-zaldehyde with the corresponding methylene compounds in the presence of catalytic amounts of piperidine and acetic acid in boiling benzene [14]. EMK 381 was obtained as reported [15]. All reagents were from Sigma–Aldrich (St. Louis, MO).

2.3. Cell treatments

U937 cells were cultured in RPMI 1640 medium supplemented with 25 mM HEPES, pH 7.3, 5% fetal calf serum, and gentamicin (50 μg/ml) (Invitrogen, Carlsbad, CA) at 37 $^\circ$C under humid 5% CO$_2$ atmosphere. Cells were grown in 75 cm^2 flasks in a volume of 15 ml up to a density of about 0.7×10^6 cells/ml and kept in fresh culture medium for 14 h before the experiments.

2.4. RNA extraction and quantitative real-time PCR analysis

Cells were lysed and total RNA was extracted using the RNA extraction kit together with DNA elimination by DNase (Promega, Madison, WI), according to the manufacturer's instructions. Two μg of RNA was used to prepare cDNAs with oligo(dT) primers and AMV reverse transcriptase (Promega). Quantitative real-time PCR (RT-PCR) was performed using the Roche Light Cycler System and the FastStart DNA Master SYBR Green I kit (Roche Diagnostics, Basel, Switzerland) as previously reported [11]. Values were normalized to the relative amounts of GAPDH cDNA. All RT-PCR measurements were performed in triplicate.

2.5. Measurement of menadione toxicity

U937 cells were grown in 96-well microtiter plates at a density of 15×10^3/well in a volume of 200 μl. The protective effect of prior 14-h incubation with 25 μM BMN compounds on survival of U937 cells exposed for 5 h to 0–60 μM menadione was quantified by colorimetric measurement of MTT reduction. Menadione (Sigma–Aldrich, St. Louis, MO) was dissolved in phosphate-buffered saline (PBS) (pH 7.3) and added to culture medium to the final concentrations as indicated. A SpectraMax Plus Reader

(Molecular Devices, Sunnyvale, CA) was used for quantification. Dose–effect analyses were performed according to [16]. The data were expressed using the median-effect equation $F_a/F_u = (D/D_m)^m$, where D is the concentration, F_a and F_u are the fractions of the cells affected and unaffected, respectively, by the concentration D, D_m is the concentration required to induce 50% cell death, and the index m is a measure of the sigmoidicity of the dose–response curve [16].

2.6. Western blotting

U937 cells ($\approx 10 \times 10^6$) were washed twice with ice-cold phosphate-buffered saline and whole cell extracts were prepared in 10 mM Tris, pH 7.4, 1% SDS, 10 mM NaF, 1 mM Na$_3$VO$_4$, and 100 μM phenylmethylsulfonyl (Sigma–Aldrich, St. Louis, MO) fluoride in a total volume of 600 μl and denatured by heating at 95 $^\circ$C for 5 min. Protein concentration in each lysate was assayed colorimetrically (Bio-Rad protein reagent; Bio-Rad, Hercules, CA), and 20 μg of protein was resolved by 10% SDS-PAGE. After electrophoresis, proteins were transferred to Hybond ECL nitro-cellulose membranes (Amersham Biosciences, UK). Membranes were blocked in Tris-buffered saline containing 5% nonfat milk for 2 h. The following antibodies were used for Western analyses: rabbit anti-HO-1 (Santa Cruz Biotechnology, Santa Cruz, CA), anti-phospho-p38, anti-phospho-c-Jun, anti-phospho-p70S6 K (Cell Signaling Technology, Beverly, MA), and anti-Nrf2 (Abcam, Cambridge, UK) at 1:100 (anti-HO-1) or 1:1000 dilution (all other antibodies) in 1× Tris-buffered saline, 0.1% Tween 20 (TTBS), and 5% BSA overnight. Rabbit anti-β-actin antibodies (Cell Signaling) at a 1:10,000 dilution in 1 × TTBS were used as a control. Appropriate horseradish peroxidase-coupled secondary goat antibodies (Dako, Glostrup, Denmark) were used for visualization using the chemiluminescent HRP substrate (Millipore, Billerica, MA) and chemiluminescence detection system (Bio-Rad, Hercules, CA). For quantification the Quantity One-4.6 software (Bio-Rad) was used.

2.7. Absorption spectra of BMN–GSH conjugates

BMNs (50 μM) were incubated with GSH (1 mM) in a total volume of 1 ml of 50 mM Tris–HCl buffer (pH 7.5) in the presence of 5% DMSO for 1 h at room temperature. Spectra were recorded using a UV–vis double-beam spectrophotometer (Safas UV mc2, Safas, Monaco). GSH and DMSO were present at the same concentration in the reference cuvette.

2.8. Liquid chromatography mass spectrometry (LC–MS) analysis of BMN–GSH conjugates

BMN compounds (1 mM) were incubated with 5 mM GSH (Sigma-Aldrich, St. Louis, MO) in a total volume of 400 μl of 50 mM Tris–HCl buffer (pH 7.5) in the presence of 10% MeOH for 1 h at room temperature. The reaction mixture was analyzed using a UPLC/MS System (Waters Acquity UPLC, Waters Corporation, Milford, MA) connected to a Waters Acquity TQD triple quadripole spectrometer, with electrospray ionization (ESI) and a Waters Acquity ELSD detector. Separations were carried out on a Waters HSS C18 (2.1 × 50 mm, 1.8 μm) column at a flow rate of 0.6 ml/min using the gradient elution from 5% water–acetonitrile to 100% acetonitrile (both containing 0.1% of formic acid) over 10 min.

3. Results

3.1. Time-course and dose dependence of AG-126 induced activation of HO-1 expression

We have previously reported that the cytoprotective protein HO-1 is highly sensitive to tyrphostin AG-126 in U937 monocytic

cells [11]. Here, we further characterized this effect by performing quantitative dose–response and time-course experiments. The HO-1 mRNA content increased in U937 cells together with AG-126 concentration up to 50 μM, to reach a maximal accumulation of about 500-fold (Fig. 1A). The HO-1 mRNA reached its maximum after a 3-h exposure to 25 μM AG-126 (Fig. 1B). The HO-1 protein level was increased up to 9 h after exposure to AG-126, reaching an approximately 10-fold increase over the basal level (Fig. 1C).

3.2. Capacity of BMNs to induce HO-1: structure–activity relationship

As a hallmark of up-regulation of cell protective systems, the capacity of a series of BMNs and structurally related compounds to affect HO-1 at both the mRNA and protein levels were examined (see Table 1). The parent benzylidenemalononitrile EMK 191 strongly activated HO-1 mRNA induction. As compared to EMK

191, in the mono-substituted BMN series with electron-withdrawing groups (NO_2, CN, halogens) in *ortho/meta/para* position and *meta*-MeO substituents (-*I* effect) increased HO-1 mRNA induction, while the electron-donating groups with strong +*R* effect in *para*-position (OH and N-morpholino) significantly decreased activity. The effect of single methoxy-group in *ortho* or *para* position was insignificant. In the series of di-substituted BMNs, the net combination of the above effects could be seen, with the exception of striking loss of activity for 3,5-dinitro-BMN EMK 281, as compared to the mono-nitro substituted EMK 491, EMK 151 and EMK 121, and compounds bearing a 4-OH group in combination with electron-withdrawing groups at the *ortho*-position to this group (4-OH,3-MeO, for EMK 031, 4-OH,3-F for EMK 211, 4-OH,3-NO_2 for EMK 071).

3.3. Effect of BMNs upon signaling pathways

A main goal of our study was to provide insights into mechanism of activation of upstream signaling systems by BMN compounds. Therefore, we examined the effects of BMNs and related compounds on the protein content and/or the phosphorylation level of key stress signaling molecules, namely the transcription factors Nrf2 and c-Jun, p70 S6 kinase (p70S6K), an mTOR substrate and key regulator of mRNA translation and p38 MAPK. As shown in Fig. 2A, a pilot study focusing on 6 BMNs showed that a majority of these compounds tend to activate Nrf2 expression and the phosphorylation of c-Jun and p38, and to reduce the phosphorylation of p70S6 K. Then, we examined the ability of BMN compounds to promote Nrf2 accumulation and c-Jun phosphorylation using an extended set of compounds (Table 1). Quantification of Western blots showed that the parent BMN (EMK 191) and the nitro-substituted BMNs (EMK 121, EMK 151, AG-126 and EMK 281) are the most effective activator of Nrf2 expression. All other substitutions attenuated the magnitude of Nrf2 accumulation whatever the presence of electron-donating and electron-withdrawing groups. As regards Nrf2 accumulation, twelve *para*-substituted BMN compounds proved effective in the following order: NO_2 > H > morpholine > MeS > CH_3 > t-Bu > MeO > F > HO > CF_3 > CN > Br, while for HO-1 gene activation, the order was: NO_2 > CN > Br > CH_3 > MeS > F > H > t-Bu > MeO ≫ HO > morpholine. The position and number of NO_2 substitution were of minor importance. In contrast, the presence of two CN groups on the lateral chain was indispensable, indicating that the Michael reaction acceptor functionality is critical for the Nrf2 activation (Table 1).

Stimulation of c-Jun phosphorylation was highly dependent on the structure of BMN compounds. In U937 cells exposed to parent BMN EMK 191, the level of phospho-c-Jun increased about 3-fold. The rank order of twelve BMN compounds as regards c-Jun activation was as follows: NO_2 > CF_3 > Br > t-Bu > MeO ≥ F ≥ CN ≥ MeS > H > CH_3 > HO ≫ morpholine. Compounds containing *para*- or *meta*-NO_2 groups, 3,5-$(MeO)_2$ (EMK 131), 4-t-Bu (EMK 241) or halogens were effective activators of c-Jun phosphorylation (FC > 5), whereas addition of multiple MeO groups (EMK 721, EMK 731, EMK 841, EMK 851, and EMK 861) was less effective. The presence of a 4-OH group (EMK 031, EMK 071, EMK 211, and EMK 871) or a 4-morpholine group (EMK 251) led to complete reduction of c-Jun phosphorylation (Table 1).

When HO-1 mRNA accumulation elicited by BMN treatment is plotted against Nrf2 content (Fig. 2B) or p-c-Jun content (Fig. 2C), a significant positive correlation can be calculated. The linear correlation coefficients (R^2) were respectively 0.346 ($n = 42$) and 0.383 ($n = 38$) whereas Pearson correlation coefficients ($\rho_{X,Y}$) were respectively 0.588 and 0.619. Of interest, BMN compounds (EMK 031, EMK 071, EMK 211, EMK 251, EMK 861, and EMK 871) that up-regulated Nrf2 accumulation but did not stimulate c-Jun
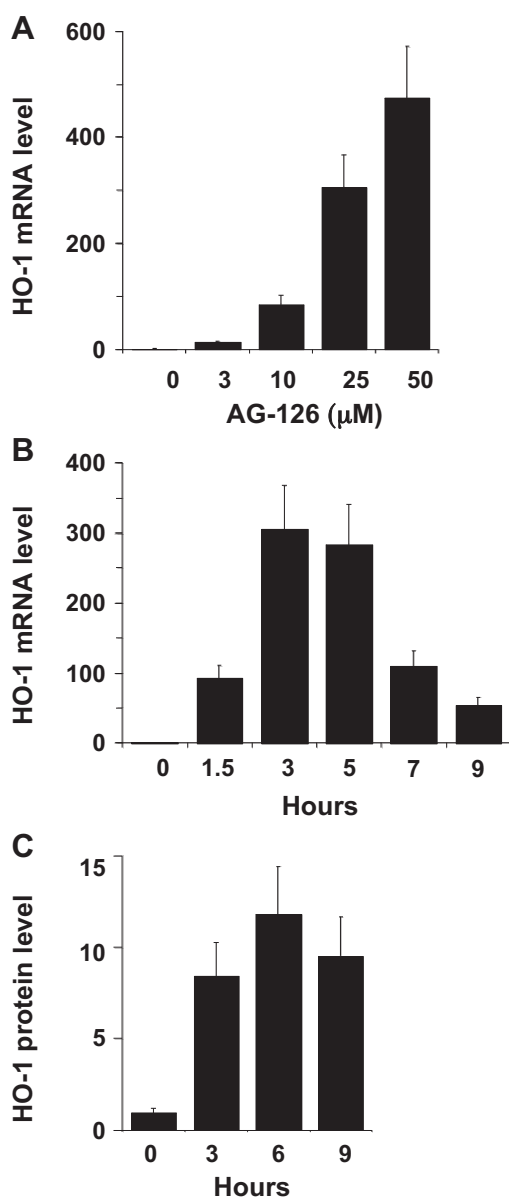

Fig. 1. HO-1 expression in U937 cells exposed to AG-126. Dose dependence (A), time-course (B) for HO-1 mRNA accumulation and time-course of HO-1 protein accumulation (C). U937 cells were incubated with 25 μM AG-126 for the indicated times (B and C) or for 3 h at the indicated concentrations (A). Each bar represents the mean ± SD of at least three independent experiments. HO-1 mRNA and protein levels in untreated cells were assigned a value of 1.

Table 1
BMN compounds examined in this study. Structure and potency to induce HO-1 and to activate Nrf2 and c-Jun.
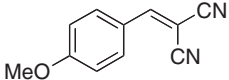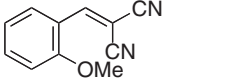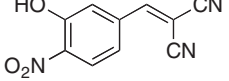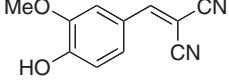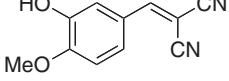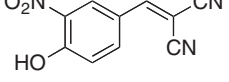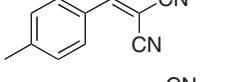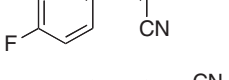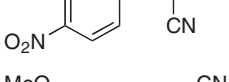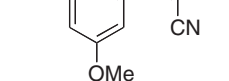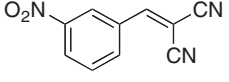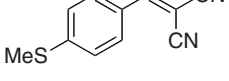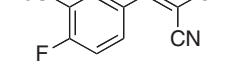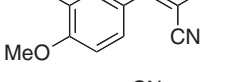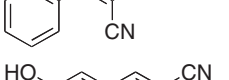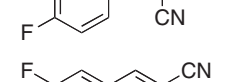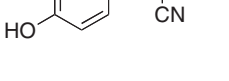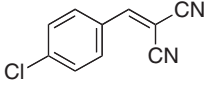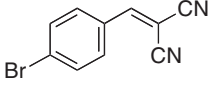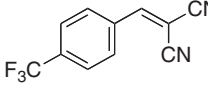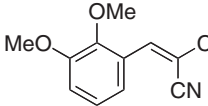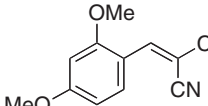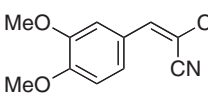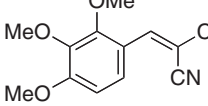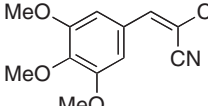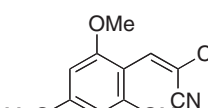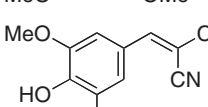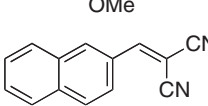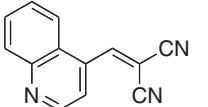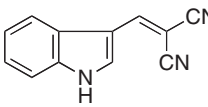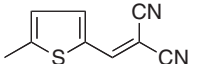
| Compounds | | Induction/activation (Fold-change) | | | |
Code	Structure	HO-1 mRNA	HO-1 protein	Nrf2	p-cJun
AG-9		76.3	ND	8.7	3.5
AG-10		28.3	ND	8.2	2.2
AG-126		307.1	8.4	13.1	5.5
EMK 031		9.4	ND	5.0	1.3
EMK 041		123.0	6.3	5.7	2.1
EMK 071		4.1	ND	7.4	0.9
EMK 081		165.7	8.0	9.2	2.5
EMK 091		127.9	ND	8.7	3.5
EMK 121		309.7	ND	15.8	13.2
EMK 131		243.4	ND	8.2	8.5
EMK 151		283.6	9.0	13.5	13.8
EMK 161		163.0	ND	9.6	3.4
EMK 171		118.3	ND	5.5	5.0
EMK 181		133.5	ND	8.8	2.8
EMK 191		98.4	ND	12.9	2.9
EMK 201		153.5	ND	7.8	3.8
EMK 211		4.5	ND	4.0	1.4

Table 1 (*Continued*)

Compounds		Induction/activation (Fold-change)			
Code	Structure	HO-1 mRNA	HO-1 protein	Nrf2	p-cJun
EMK 221		188.1	5.4	6.4	5.5
EMK 231		135.7	ND	5.8	5.1
EMK 241		81.3	ND	8.9	5.3
EMK 251		10.0	ND	9.7	1.1
EMK 281		145.4	7.0	12.4	12.8
EMK 301		7.7	ND	1.5	8.8
EMK 311		1.6	ND	1.7	6.4
EMK 321		1.3	ND	1.1	1.9
EMK 381		1.0	ND	1.0	1.5
EMK 421		169.5	9.6	7.0	3.6
EMK 431		246.4	8.3	ND	ND
EMK 441		276.3	12.1	6.5	4.0
EMK 461		232.3	5.7	11.5	29.6
EMK 471		93.2	6.8	6.4	2.7
EMK 491		245.5	9.1	4.8	7.2
EMK 511		270.6	10.9	ND	ND
EMK 531		260.6	11.5	ND	ND
EMK 591		272.5	14.2	4.9	3.5

Table 1 (Continued)

Compounds		Induction/activation (Fold-change)			
Code	Structure	HO-1 mRNA	HO-1 protein	Nrf2	p-cJun
EMK 611		ND	9.4	4.3	3.8
EMK 621		240.5	6.0	4.8	8.3
EMK 661		ND	ND	5.3	11.7
EMK 711		136.4	9.6	4.5	2.1
EMK 721		25.7	2.9	4.3	1.3
EMK 731		31.5	4.1	4.8	1.6
EMK 841		31.3	6.3	4.2	1.2
EMK 851		40.4	4.0	3.5	1.5
EMK 861		2.1	1.3	2.1	1.1
EMK 871		2.0	1.7	2.6	1.2
EMK 991		ND	6.9	4.3	3.2
EMK 1041		ND	ND	7.1	5.0
EMK 1051		ND	1.0	2.3	1.0
EMK 1071		40.5	2.9	7.9	1.8

U937 cells were exposed to the indicated chemicals (25 μM) for 3 h. Relative mRNA and protein levels were measured by RT-PCR and Western blotting, respectively. The mRNA and protein (phosphoprotein) levels in untreated cells were assigned a value of 1. Data represent the mean of at least three independent experiments. BMN compounds referred to here as EMK 031, EMK 041, EMK 071, EMK131, and EMK 251 are also known as tyrphostins A16, A15, A19, A2, and A6, respectively [1]. ND, not done.
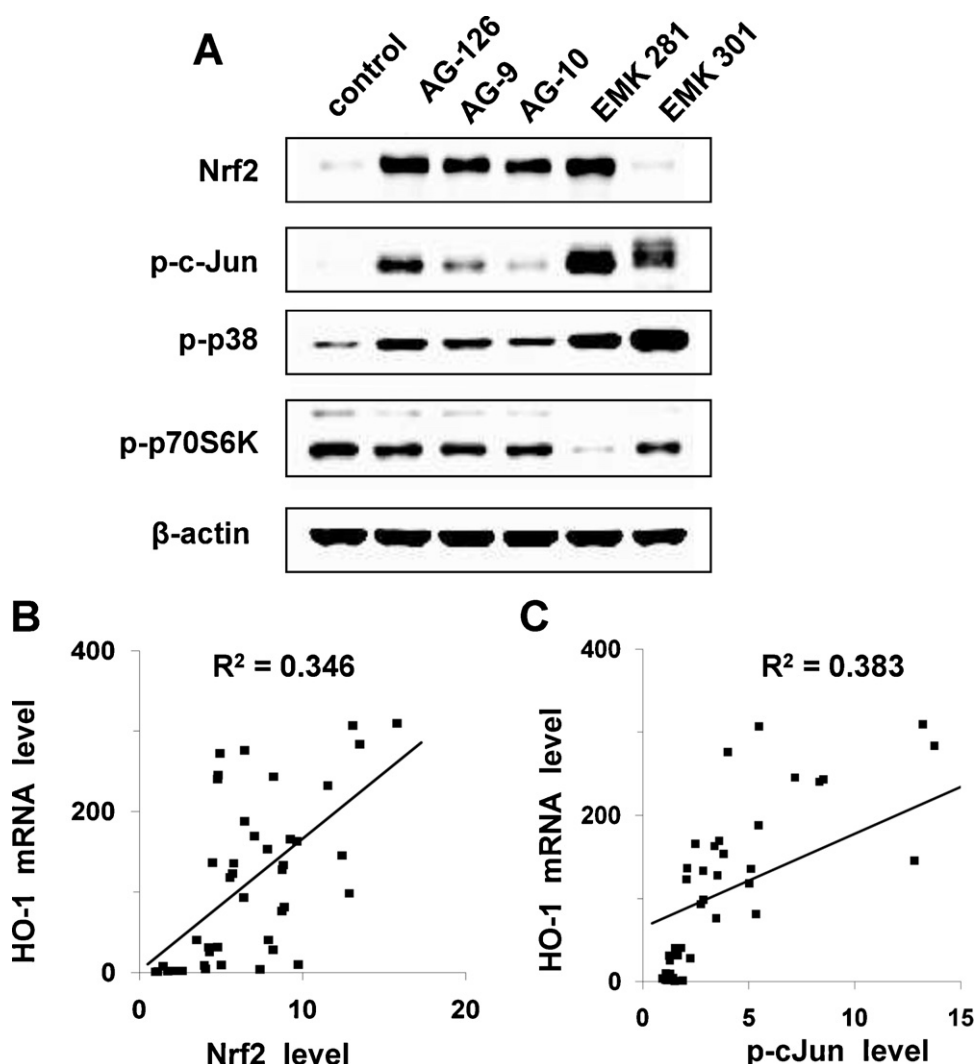
Fig. 2. Activation of signaling systems by selected BMNs or structurally similar compounds. (A) Representative Western blot image. U937 cells were incubated with BMNs (25 μM) for 3 h. Whole cell lysates were analyzed by immunoblotting with Nrf2, phospho-cJun, phospho-p38, phospho-p70S6K, and β-actin antibodies. (B) Relative induction of HO-1 mRNA plotted against Nrf2 level. (C) Relative induction of HO-1 mRNA plotted against p-c-Jun level. Western blot or RT-PCR quantification data of three independent experiments are shown. HO-1 mRNA and protein levels in untreated cells were assigned a value of 1.

phosphorylation were weak HO-1 inducers. Conversely, compounds which actively stimulated both c-Jun phosphorylation and Nrf2 accumulation (e.g. BMNs containing a NO_2 group) are very potent activators of HO-1 gene expression. Altogether, these data suggest that parallel actions of Nrf2 and p-c-Jun is a prerequisite for full-scale HO-1 induction, and subsequently for accumulation of HO-1 protein.

Activation of p38 phosphorylation was markedly stimulated by compounds bearing NO_2- and halogen benzene ring substituents (Supplemental Table 1). Regarding p-p70S6 K, its level was strongly reduced (FC = 0.16) in cells exposed to EMK 281 whereas FC was between 0.4 and 0.5 for EMK 311, EMK 431, EMK 211, EMK 491, EMK 621, and EMK 151 (see Fig. 2A and Supplemental Table 1). However, only slight to moderate correlation was noted between accumulation of HO-1 mRNA and either p-p38 or p-p70SK content in U937 cells treated with BMNs (data not shown).

3.4. Protective effects of BMN compounds upon oxidative stress

To generate oxidative stress, we exposed U937 cells to menadione, which induces cell death through superoxide generation and depletion of intracellular SH-containing molecules. Twelve compounds with different capacity to induce HO-1 were selected. In control experiments, survival of U937 cells decreased as menadione concentration increased, and at concentration over 40 μM almost no cell survived. Fig. 3A shows a representative plot of the protective effect of prior incubation with AG-126 on survival of U937 cells exposed to menadione. Cell death reached 95% after exposure to 30 μM menadione, but declined to 55% when cells were pretreated with 25 μM AG-126 for 14 h. Menadione toxicity on U937 cells was quantified by calculating its median-effect concentration (D_m) upon 5-h exposure (Fig. 3B) was 13.3 ± 1.9 μM. Interestingly, prior incubation of U937 cells with AG-126 for 6, 14 or 22 h caused a D_m increase of 34, 66 or 68%, respectively. U937 cells were also pretreated with different BMN compounds (25 μM) for 14 h prior to exposure to menadione for 5 h. Even though they are structurally different from AG-126, EMK 121 and EMK 201 had a similar protective effect whereas BMN compounds with MeO substitutions (EMK 041, EMK 131, EMK 721, EMK 731, EMK 841) (Table 2) were weaker protectors. Subsequent analysis revealed a significant correlation between HO-1 induction and the protective properties of the analyzed BMN compounds. Pearson correlation coefficients ($\rho_{X,Y}$) between Dm increase and induction of HO-1 at the mRNA and protein levels, were 0.683 ($n = 12$) and 0.784 ($n = 9$), respectively, and the linear correlation coefficients (R^2) were 0.467 ($p < 0.02$) and 0.615 ($p < 0.02$), respectively (Fig. 3C and D).
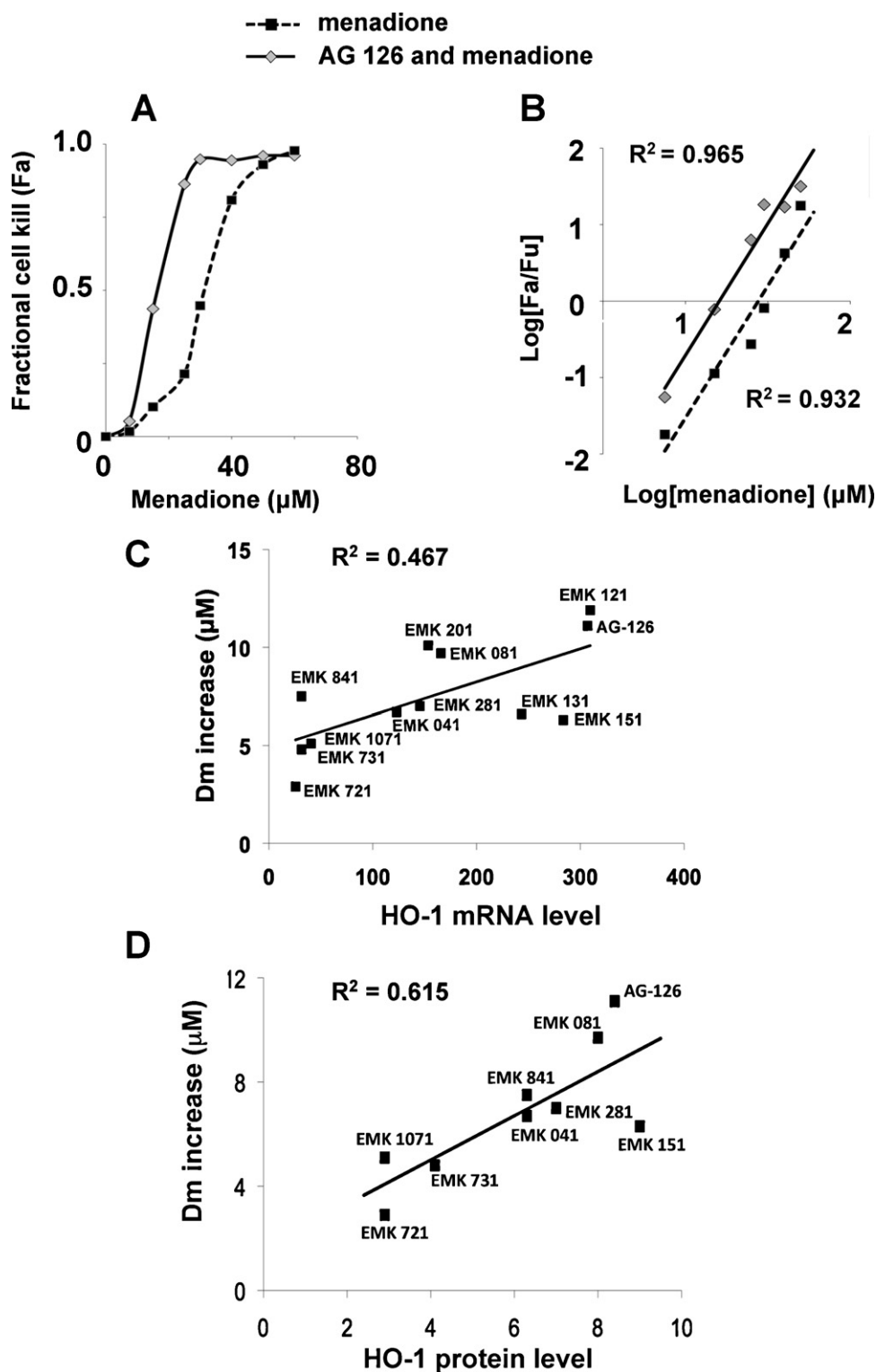
Fig. 3. Protective effects of BMNs upon oxidative stress. (A) Fraction of necrotic cells (F_a) plotted against menadione concentration. Cells were exposed to menadione for 5 h after being pre-treated or not with 25 μM AG-126 (14 h). (B) Analysis of the above data by the median effect plot. F_u is the fraction of unaffected cells. The results are analyzed by plotting log (F_a/F_u) with respect to log of menadione concentration (0–60 μM). (C) Correlations between HO-1 mRNA accumulation or (D) HO-1 protein content and the median concentration values (D_m) of BMNs (12 and 9 compounds for C and D, respectively). D_m is the concentration of menadione required to produce a 50% toxic effect, i.e., when $F_a = F_u$. Each D_m value represents the mean of three independent experiments.

3.5. Spectroscopic evidence for reactivity of AG-126 with GSH

In cells of different types, activation of redox-sensitive signaling pathways is triggered mainly by modification of sensitive cysteine residues on specific cellular targets. It was shown that chlorobenzylidene malononitriles referred to in this study as EMK 531 and EMK 611 conjugate with GSH, the most abundant cellular thiol compound [17]. UV–vis spectrum of AG-126 (50 μM) with GSH (1 mM) in 50 mM Tris HCl buffer (pH 7.4) showed a slight hypsochromic shift from 281 to 278 nm with concomitant increase of intensity of the absorption maximum (Fig. 4). These spectral alterations suggest that AG-126 forms a conjugate with GSH.

Table 2
Protective effects of BMN compounds upon menadione toxicity.

Compounds	D_m ($\pm$SD)	D_m increase (μM)
AG-126	24.4 ± 2.5	11.1
EMK 041	20.0 ± 2.2	6.7
EMK 081	23.0 ± 2.3	9.7
EMK 121	25.2 ± 2.7	11.9
EMK 131	19.9 ± 2.1	6.6
EMK 151	19.6 ± 2.2	6.3
EMK 201	23.4 ± 2.4	10.1
EMK 281	20.3 ± 1.9	7.0
EMK 721	16.2 ± 1.8	2.9
EMK 731	18.1 ± 2.5	4.8
EMK 841	20.8 ± 2.0	7.5
EMK 1071	18.4 ± 1.9	5.1

U937 cells were exposed or not to the indicated BMN compounds (25 μM) for 14 h prior to treatment with menadione (0–60 μM) for an additional 5-h period. The data are expressed as the variation of the median-effect concentration (D_m) in BMN preconditioned cells relative to untreated cells, and are the mean of at least three independent experiments. The D_m value for cells exposed to menadione alone was 13.3 ± 1.9 μM.

3.6. Correlations between chemical activity of BMN compounds and HO-1 mRNA induction

The reactivity of some BMNs and related Michael acceptors toward thiols has previously been studied [17,18]. The reaction proceeds via a fast reversible addition of a thiol to the conjugated system. Equilibrium constants for reactions with n-butanethiol of BMN derivatives referred here to as EMK 031, EMK 721, AG-9, EMK 081, EMK 471, EMK 491, EMK 191, EMK 231, EMK 621, EMK 441, EMK 531, EMK 151, and EMK 121 range from 0.13 to 12.0×10^2 (M^{-1}) (25 °C, pH 7.0) [18]. We analyzed the correlation between BMN reaction rates with thiols by plotting the equilibrium constant for the reactions between BMNs and n-butanethiol [18] versus the capacity to induce HO-1 gene expression (our data from Table 1). As shown in Fig. 5A, there is a clear correlation between these two parameters ($R^2 = 0.674$, $\rho_{X,Y} = 0.821$, $n = 14$).

Moreover, as shown in Fig. 5B, there is a positive correlation between the hydrolysis rate of BMNs [19] and the capacity to induce HO-1 mRNA expression ($R^2 = 0.742$, $\rho_{X,Y} = 0.861$, $n = 12$). Calculated half-lives of these BMN compounds in aqueous solution range from 2.5 min to 38.3 h. Surprisingly, the short lifespan of BMN compounds in water did not reduce their capacity to induce HO-1 mRNA. Thus, the compounds with a short half-life such as EMK 121, EMK 151 and EMK 531 (calculated $t_{1/2}$ = 2.5, 3.2 and 9.7 min, respectively) were the most effective activators of HO-1 gene expression.

3.7. LC–MS analysis of BMN adducts with GSH

In order to further characterize GSH conjugates with BMNs, we analyzed the reaction mixtures of a selection of BMNs with reduced GSH (1 h, 25 °C) by LC–MS using electrospray ionization (ESI) in positive and negative mode. The compounds tested (AG-126, EMK 131, EMK 721, EMK 731, and EMK 1071) were selected because they differently stimulate HO-1 expression and activate upstream signaling systems (Table 1). As shown in Fig. 6A, evaporative light scattering detector (ELSD) revealed a single product of the reaction between AG-126 and GSH eluting at 1.50 min. Detailed ESI-MS2- analysis produced a peak with an m/z value of 828.5, corresponding to the conjugate of AG-126 with two equivalents of GSH and gave rise to fragments at 521 (R-GSH) and 306 (GSH). The thiophene malononitrile EMK 1071, after reaction with GSH, produced a compound with an ELSD retention time of 2.00 min. ESI-MS2-analysis showed two major peaks corresponding to the mono- and di-charged ions (482.2 and 241.7), suggesting
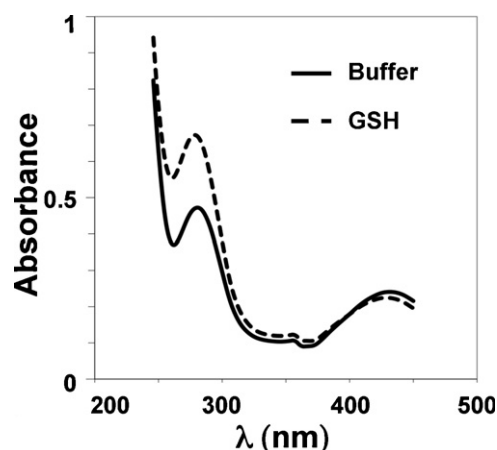
Fig. 4. Spectrophotometric analysis of AG-126 reaction with GSH. AG-126 (50 μM) was incubated with (dotted line) or without (solid line) 1 mM GSH in 50 mM Tris–HCl buffer containing 5% of DMSO (pH 7.5) for 1 h at room temperature.

that this compound reacts with a single molecule of GSH (Fig. 6B). Likewise, reaction of EMK 131 (3,4-$(MeO)_2$ BMN) with GSH, gave a single product with elution retention time of 1.64 min. ESI-MS2 analysis revealed an m/z value of 827.5 corresponding to conjugate between EMK 131 and two GSH (Fig. 6C). As regards EMK 721 (2,4-$(MeO)_2$ BMN), ELSD analysis detected a single product resulting from conjugation of one GSH and one EMK 721 molecule (m/
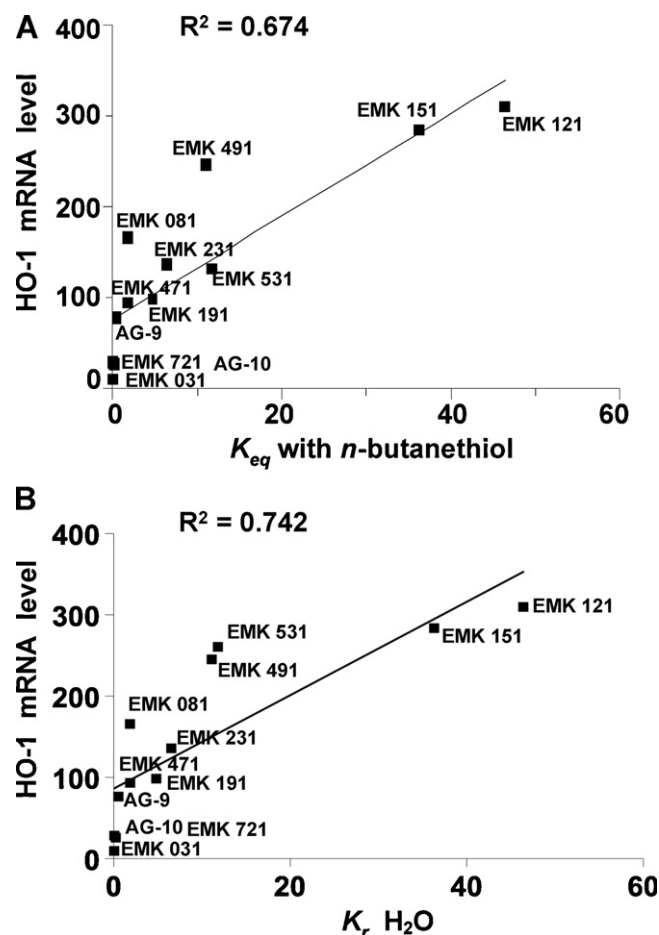
Fig. 5. Correlation between HO-1 gene expression and chemical properties of BMN compounds. The relative levels of HO-1 mRNA (data from Table 1) were plotted against equilibrium constants ($K_{eq} \times 10^{-2}$) for reactions with n-butanethiol [18] (A) and BMN hydrolysis first-order constants ($k_{H_2O} \times 10^4$) [19] (B).
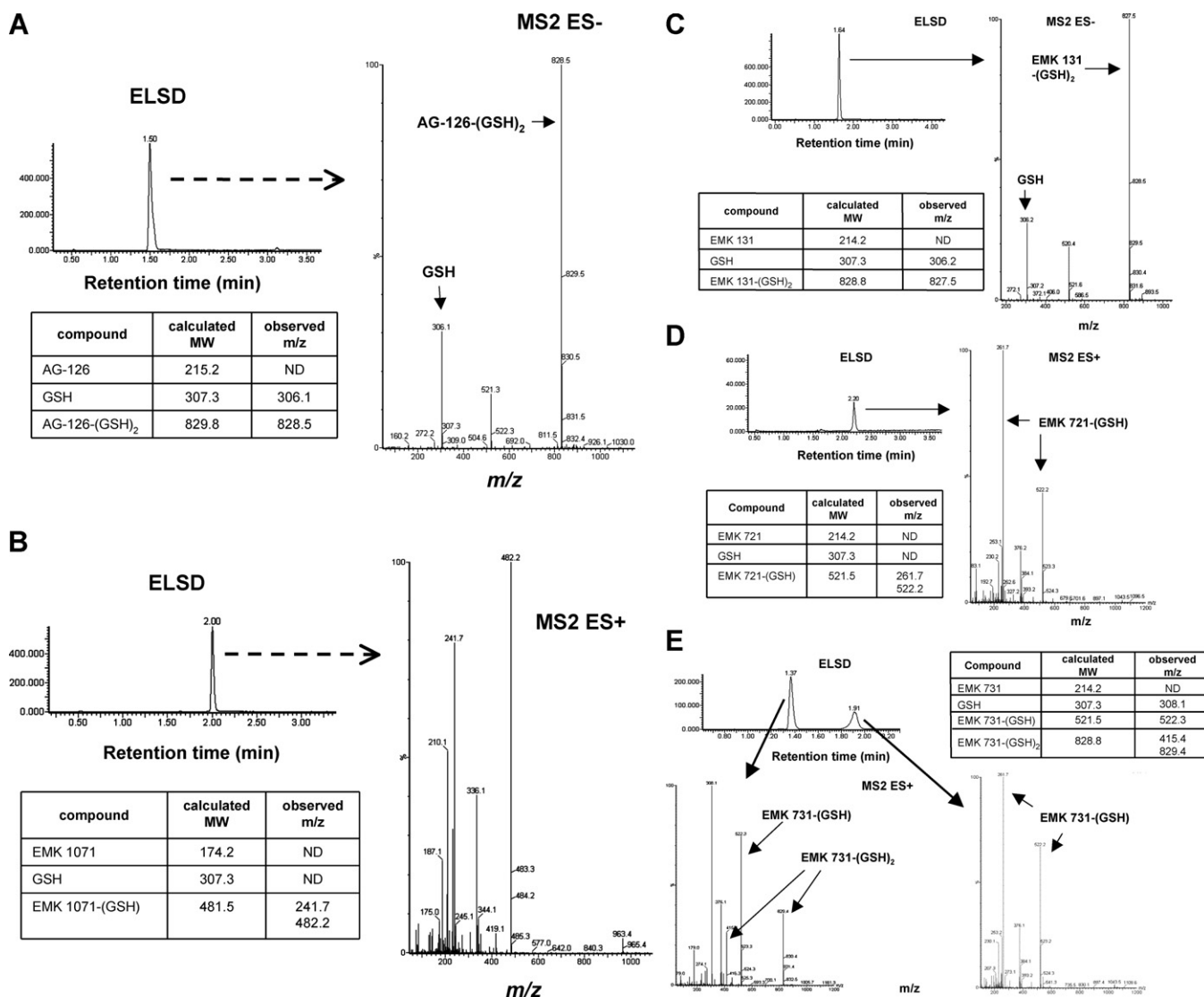
Fig. 6. LC–MS analysis of adducts between GSH and BMNs. ELSD chromatograms and subsequent ESI-MS2 analysis of the reaction products. Bottom panels compare the experimental m/z and calculated MW values of initial compounds and expected GSH conjugates. Compounds were incubated with 5 mM GSH in 50 mM Tris–HCl buffer containing 10% of MeOH (pH 7.5) for 1 h at room temperature. The incubation of AG-126 (A) and EMK 1071 (B) with GSH resulted in generation of single ELSD detectable products with retention time 1.50 and 2.00 min, respectively. ESI-MS2 analyses suggest that AG-126 conjugates with two GSH equivalents whereas EMK 1071 conjugates with one GSH molecule. The product of EMK 131 (C) and EMK 721 (D) reactions with GSH were revealed as a single peaks (ELSD retention times 1.64 and 2.20 min, respectively) corresponding to BMN adducts with a one molecule of GSH. The incubation of EMK 731 (E) with GSH resulted in the generation of two products revealed by ELSD as peaks at retention times of 1.37 and 1.91 min. ESI-MS2 analysis suggests that the first peak corresponds to EMK 731 conjugated with two GSH equivalents whereas the second one corresponds to EMK 731 conjugate with a single GSH molecule.

$z = 522.2$) (Fig. 6D). Lastly, the reaction between EMK 731 (3,4-(MeO)$_2$ BMN) and GSH generated two products with elution retention time of 1.4 and 1.9 min consistent with the addition of two ($m/z = 829.4$) and one ($m/z = 522.3$) molecule(s) of GSH to one molecule of EMK 731, respectively (Fig. 6E). It is worth noting that LC–MS analysis performed after 1-h and 24-h incubation of AG-126 with GSH revealed the same composition of the reaction mixture (data not shown), suggesting that these conjugates of BMN with GSH are thermodynamically stable.

4. Discussion

In a previous study, we showed that BMN compounds are potent activators of HO-1 expression [11]. Thus, in U937 cells exposed to AG-126, the level of HO-1 mRNA increased to more than 300 times the basal level, as compared with the synthetic triterpenoid CDDO-imidazolide which stimulates HO-1 mRNA

expression 90-fold [20]. Here, we point to a significant correlation between BMN-mediated HO-1 induction and decrease in menadione-induced toxicity, suggesting that HO-1 up-regulation is an indicator of drug efficacy. In addition, our investigation of the structure–activity relationship of 49 BMNs points out structure substitutions that determine specific responsiveness of major signaling pathways.

HO-1 gene expression is activated mainly at the transcriptional level in various cell types by a broad spectrum of chemical and physical agents including heat shock, ultraviolet light, hypoxia, cytokines, reactive oxygen and nitrogen species, and xenobiotics [21,22]. The regulation of HO-1 expression is mediated by a complex network of transcriptional regulators acting on many responsive elements located in the promoter region of the HO-1 gene: antioxidant response element (ARE), Maf recognition element (MARE), hypoxia response elements (HREs), heat shock element (HSE), and multiple binding sites for transcription factors
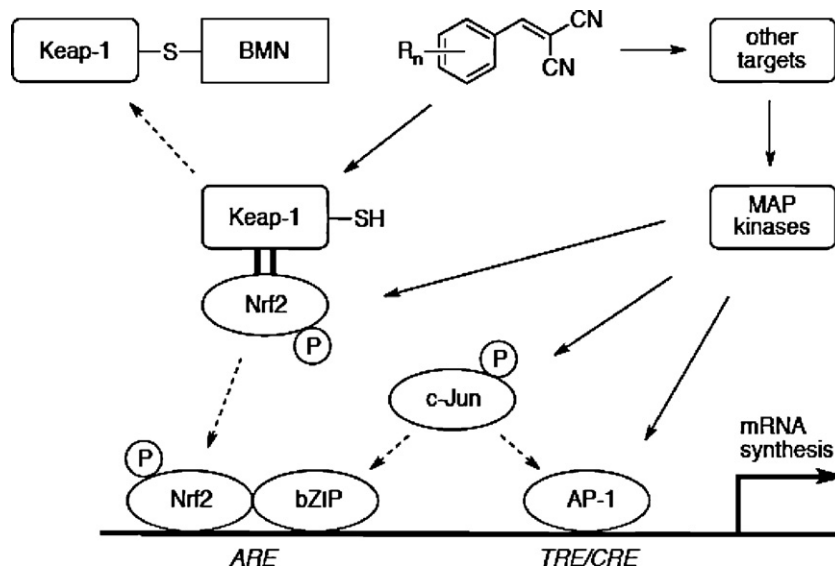
Fig. 7. Scheme of a proposed mechanism of BMN-dependent signaling and regulation of HO-1 gene expression. In the absence of BMN, the thiol-rich sensor protein Keap1 retains Nrf2 in the cytoplasm where it is targeted for ubiquity-mediated degradation. BMN compounds alkylate reactive SH-groups of Keap1 resulting in Nrf2 dissociation, nuclear translocation and binding to ARE regulatory elements in heteromeric combination with bZIP family transcription factors (c-Jun, small Maf proteins, ATF4). In parallel, BMN compounds can modify other regulatory proteins, resulting in up-regulation of MAP kinases and AP-1 family transcription factors. MAP kinases can regulate Nrf2 stability and induce gene expression via the AP-1 binding sites TPA-responsive element (TRE) and c-AMP-responsive element (CRE). Multiple copies of AP-1 binding sites are present in the regulatory region of HO-1 gene.

AP-1, C/EBP, STAT, and NF-κB. In brief, the master regulator Nrf2 plays a central role in induction of HO-1 in partnership with other transcription factors including small Maf proteins, c-Jun and ATF4 [23–26].

Our structure–activity relationship analysis shows that BMN compounds have different structural requirements for activation of Nrf2 and c-Jun cellular signaling pathways (Table 1). It is interesting to note that with the exception of EMK 841, none of the 14 BMNs displaying either Nrf2 or p-c-Jun low expression (FC ≤ 1.7) was found to elicit robust (FC > 10) HO-1 mRNA induction (Table 1). These observations suggest that the parallel increase in cellular Nrf2 and p-c-Jun is a prerequisite for full-scale HO-1 gene induction by BMNs. This assertion is supported by our previous observation that U937 cell treatment with tyrphostin AG-126 and synthetic NO donor DPTA-NO, a potent c-Jun activator, had a cumulative effect on expression of the ferritin H and IL-8 genes [11] which, like HO-1, are under the control of Nrf2/ARE and AP-1 signaling [27,28]. Nrf2/ARE signaling can be activated through Nrf2 phosphorylation by MAP kinases and other regulatory protein kinases that facilitate Nrf2 nuclear translocation [29,30]. It is therefore possible that HO-1 induction by BMN compounds is mediated by JNK-dependent phosphorylation of Nrf2, as previously shown for PC-3 cells exposed to isothiocyanates [29]. As summarized in the scheme proposed in Fig. 7, interplay between different signaling networks shows that the BMN-induced activation of HO-1 expression can be explained by the binding of the Nrf2-c-Jun complex to ARE regulatory sequences located in the enhancer region [29,30].

Nrf2 functional activity is regulated negatively by Keap1, a cytoplasmic factor that binds Nrf2 and the actin cytoskeleton, and has ubiquitin ligase adaptor activity. Association of Keap1 with Nrf2 retains the latter in the cytoplasm and promotes its rapid proteosomal degradation. Keap1 contains several critical thiol groups, particularly Cys^{151}, Cys^{273}, Cys^{278}, and their oxidation by reactive oxygen species or alkylation by electrophiles enables dissociation and nuclear translocation of Nrf2 [31–34]. Chemical substances activating Keap1/Nrf2 pathway were classified by Talalay and co-workers as 10 distinct groups that include quinones, isothiocyanates, dimercaptans, heavy metals, and

various Michael reaction acceptors like olefins conjugated to electron-withdrawing groups [35,36]. A common feature of these structurally different compounds is their high reactivity with sulfhydryl groups.

Our results indicate that potency of BMN compounds to induce HO-1 mRNA induction is related to their properties of Michael reaction acceptors. Thus, the presence of two strong electron-withdrawing CN groups conjugated to a C=C bond, is a critical requirement for transcriptional activation of HO-1 gene. Furthermore, our data showing that reactivity of BMNs and related Michael acceptors with thiols is correlated with their capacity to induce HO-1 expression, suggest that BMN compounds can modify Keap1 and others cytoplasmic regulatory factors by linking to their critical protein sulfhydryl groups. Binding to Keap-1 would promote release and translocation of Nrf2 to the nucleus where it forms heterodimers with partner proteins (e.g. c-Jun), binds to the ARE, and activate gene expression. In addition, our finding that BMN reactivity with GSH correlates with the rate of HO-1 mRNA induction is in good agreement with previous results obtained by Talalay's group showing that the reactivity of benzylideneketone acceptors with sulfhydryl reagents is the major factor that determines their potency to induce cell protective genes [36]. Further, a quantum chemical study established significant structure–activity relationships between electron-acceptor properties of triterpenoids and their biological potencies [37].

LC–MS analysis revealed that reaction of GSH with BMN compounds could generate two types of conjugates, one with two GSH molecules and another with one GSH molecule. Remarkably, AG-126 and EMK 131 which generate di(GSH) conjugates, induced HO-1 mRNA expression and c-Jun activation more potently than EMK 721, EMK 1071, and EMK 731 which generate mono-GSH conjugates. The ability of several BMN compounds to generate conjugates with two GSH equivalents suggests they can yield intra-or inter-molecular bridges between low- or high-molecular weight thiols. It is tempting to speculate that GSH, the most abundant cellular thiol, may serve as a carrier molecule for BMNs, protecting them from a simple hydrolysis, and liberating them upon cell demands.

A large body of experimental data shows that under physiological conditions, BMN compounds are able to stimulate the resistance of cells and tissues against different harmful challenges. For example, tyrphostin AG-1714 (4-nitrobenzylidene malononitrile, referred to here as EMK 121) provides significant protection against mortality induced by chemotherapy with cisplatin and doxorubicin in animals and in cell cultures [7]. Remarkably, AG-1714 stimulates resistance of healthy tissues to chemotherapy without protecting malignant tissues against drug-mediated suppression [7]. This selectivity may be associated with increased basal HO-1 expression in various tumor cells [22]. Experiments performed in vivo showed that tyrphostin AG-126 reduced development of pneumococcal meningitis, kidney acute injury and dysfunction after ischemia and reperfusion, development of acute pancreatitis, consequences of spinal cord trauma, and mitochondria-mediated 7-ketocholesterol toxicity [6,10,38–41]. Our findings that BMN compounds are activators of cell protection may provide clues to development of new drugs that mimic the protective response.

In conclusion, our study discloses that full activation of HO-1 expression by BMNs requires parallel up-regulation of two major signaling pathways, the Nrf2/Keap-1 system and the c-Jun/JNK pathway. This finding provides a possible tool for pharmacological modulation of intercellular signaling. Many short-distance signaling molecules like prostaglandins, NO, regulatory peptides, and cytokines activate JNK MAP kinases and c-Jun phosphorylation. It is thus likely that BMN compounds dedicated to Nrf2 activation will up-regulate protective systems exclusively in tissues that produce c-Jun-activating signaling molecules. According to these guidelines, the most suitable molecules are 4-morphlino BMN (EMK 251), 4-OH BMN (AG-10, EMK 031, EMK 071) and thiophene malononitrile EMK 1071. However, a potential drawback of AG-10 is its adverse effect, as a phenolic compound, on mitochondrial membrane polarity [3]. Nonetheless, because of the different capacities of BMN hydrolysis products to cross membranes, we suggest that BMNs chiefly react with molecular targets located in proximity to vasculature.

Acknowledgments

Appendix A. Supplementary data

Supplementary data associated with this article can be found, in the online version, at doi:10.1016/j.bcp.2011.05.028.

References

[1] Gazit A, Yaish P, Gilon C, Levitzki A. Tyrphostin I: synthesis and biological activity of protein tyrosine kinase inhibitors. J Med Chem 1989;32:2344–52.
[2] Levitzki A, Mishani E. Tyrphostins and other tyrosine kinase inhibitors. Annu Rev Biochem 2006;75:93–109.
[3] Sagara Y, Ishige K, Tsai C, Maher P. Tyrphostins protect neuronal cells from oxidative stress. J Biol Chem 2002;277:36204–15.
[4] Soltoff SP. Evidence that tyrphostins AG10 and AG18 are mitochondrial uncouplers that alter phosphorylation-dependent cell signaling. J Biol Chem 2004;279:10910–8.
[5] Novogrodsky A, Vanichkin A, Patya M, Gazit A, Osherov N, Levitzki A. Prevention of lipopolysaccharide-induced lethal toxicity by tyrosine kinase inhibitors. Science 1994;264:1319–22.
[6] Hanisch UK, Prinz M, Angstwurm K, Häusler KG, Kann O, Kettenmann H, et al. The protein tyrosine kinase inhibitor AG126 prevents the massive microglial cytokine induction by pneumococcal cell walls. Eur J Immunol 2001;31:2104–15.
[7] Novogrodsky A, Weisspapir M, Patya M, Meshorer A, Vanichkin A. Tyrphostin 4-nitrobenzylidene malononitrile reduces chemotherapy toxicity without impairing efficacy. Cancer Res 1998;58:2397–403.
[8] Vanichkin A, Patya M, Lagovsky I, Meshorer A, Novogrodsky A. 4-Nitrobenzylidene malononitrile reduces apoptosis-mediated liver injury in mice. J Hepatol 2002;36:631–6.
[9] Kann O, Hoffmann A, Schumann RR, Weber JR, Kettenmann H, Hanisch UK. The tyrosine kinase inhibitor AG126 restores receptor signaling and blocks release functions in activated microglia (brain macrophages) by preventing a chronic rise in the intracellular calcium level. J Neurochem 2004;90:513–25.
[10] Chatterjee PK, Patel NS, Kvale EO, Brown PA, Stewart KN, Britti D, et al. The tyrosine kinase inhibitor tyrphostin AG126 reduces renal ischemia/reperfusion injury in the rat. Kidney Int 2003;64:1605–19.
[11] Turpaev K, Drapier JC. Stimulatory effect of benzylidenemalononitrile tyrphostins on expression of NO-dependent genes in U-937 monocytic cells. Eur J Pharmacol 2009;606:1–8.
[12] Kunnumakkara AB, Anand P, Aggarwal BB. Curcumin inhibits proliferation, invasion, angiogenesis and metastasis of different cancers through interaction with multiple cell signaling proteins. Cancer Lett 2008;269:199–225.
[13] Sporn MB, Suh N. Chemoprevention: an essential approach to controlling cancer. Nat Rev Cancer 2002;2:537–43.
[14] Harper DAR, Steenson BE. Preparation of α,β-unsaturated sulfones by the Knoevenagel method. Synthesis 1980;806–7.
[15] Bumagin NA, Andryukhova NP, Beletskaya IP. Arylation of acrylonitrile with aryl halides catalyzed by palladium complexes. Dokl Akad Nauk SSSR 1990;313:107–9.
[16] Chou TC, Talalay P. Quantitative analysis of dose–effect relationships: the combined effects of multiple drugs or enzyme inhibitors. Adv Enzyme Regul 1984;22:27–55.
[17] Rietveld EC, Hendrikx MM, Seutter-Berlage F. Glutathione conjugation of chlorobenzylidene malononitriles in vitro and the biotransformation to mercapturic acids in rats. Arch Toxicol 1986;59:228–34.
[18] Pritchard RB, Lough CE, Currie DJ, Holmes HL. Equilibrium reactions of n-butanethiol with some conjugated heteroenoid compounds. Can J Chem 1968;46:775–81.
[19] Pritchard RB, Lough CE, Reesor JB, Holmes HL, Currie DJ. The relative rates of reaction of potassium cyanide and water with substituted benzalmalononitriles. Can J Chem 1967;45:775–7.
[20] Liby K, Hock T, Yore MM, Suh N, Place AE, Risingsong R, et al. The synthetic triterpenoids, CDDO and CDDO-imidazolide, are potent inducers of heme oxygenase-1 and Nrf2/ARE signaling. Cancer Res 2005;65:4789–98.
[21] Ryter SW, Alam J, Choi AM. Heme oxygenase-1/carbon monoxide: from basic science to therapeutic applications. Physiol Rev 2006;86:583–650.
[22] Was H, Dulak J, Jozkowicz A. Heme oxygenase-1 in tumor biology and therapy. Curr Drug Targets 2010;11:1551–70.
[23] Copple IM, Goldring CE, Kitteringham NR, Park BK. The Nrf2-Keap1 defense pathway: role in protection against drug-induced toxicity. Toxicology 2008;246:24–33.
[24] Levy S, Jaiswal AK, Forman HJ. The role of c-Jun phosphorylation in EpRE activation of phase II genes. Free Radic Biol Med 2009;47:1172–9.
[25] Jaiswal AK. Nrf2 signaling in coordinated activation of antioxidant gene expression. Free Radic Biol Med 2004;36:1199–207.
[26] Lee AC, Murray M. Up-regulation of human CYP2J2 in HepG2 cells by butylated hydroxyanisole is mediated by c-Jun and Nrf2. Mol Pharmacol 2010;77:987–94.
[27] Pietsch EC, Chan JY, Torti FM, Torti SV. Nrf2 mediates the induction of ferritin H in response to xenobiotics and cancer chemopreventive dithiolethiones. J Biol Chem 2003;278:2361–9.
[28] Loboda A, Stachurska A, Florczyk U, Rudnicka D, Jazwa A, Wegrzyn J, et al. HIF-1 induction attenuates Nrf2-dependent IL-8 expression in human endothelial cells. Antioxid Redox Signal 2009;11:1501–17.
[29] Xu C, Yuan X, Pan Z, Shen G, Kim JH, Yu S, et al. Mechanism of action of isothiocyanates: the induction of ARE-regulated genes is associated with activation of ERK and JNK and the phosphorylation and nuclear translocation of Nrf2. Mol Cancer Ther 2006;5:1918–26.
[30] Anwar AA, Li FY, Leake DS, Ishii T, Mann GE, Siow RC. Induction of heme oxygenase 1 by moderately oxidized low-density lipoproteins in human vascular smooth muscle cells: role of mitogen-activated protein kinases and Nrf2. Free Radic Biol Med 2005;39:227–36.
[31] Sekhar KR, Rachakonda G, Freeman ML. Cysteine-based regulation of the CUL3 adaptor protein Keap1. Toxicol Appl Pharmacol 2010;244:21–6.
[32] Dinkova-Kostova AT, Holtzclaw WD, Kensler TW. The role of Keap1 in cellular protective responses. Chem Res Toxicol 2005;18:1779–91.
[33] Wakabayashi N, Dinkova-Kostova AT, Holtzclaw WD, Kang MI, Kobayashi A, Yamamoto M, et al. Protection against electrophile and oxidant stress by induction of the phase 2 response: fate of cysteines of the Keap1 sensor modified by inducers. Proc Natl Acad Sci USA 2004;101:2040–5.
[34] Fourquet S, Guerois R, Biard D, Toledano MB. Activation of NRF2 by nitrosative agents and H₂O₂ involves KEAP1 disulfide formation. J Biol Chem 2010;285:8463–71.
[35] Dinkova-Kostova AT, Fahey JW, Talalay P. Chemical structures of inducers of nicotinamide quinone oxidoreductase 1 (NQO1). Methods Enzymol 2004;382:423–48.
[36] Dinkova-Kostova AT, Massiah MA, Bozak RE, Hicks RJ, Talalay P. Potency of Michael reaction acceptors as inducers of enzymes that protect against carcinogenesis depends on their reactivity with sulfhydryl groups. Proc Natl Acad Sci USA 2001;98:3404–9.

[37] Bensasson RV, Zoete V, Berthier G, Talalay P, Dinkova-Kostova AT. Potency ranking of triterpenoids as inducers of a cytoprotective enzyme and as inhibitors of a cellular inflammatory response via their electron affinity and their electrophilicity index. Chem Biol Interact 2010;186:118–26.

[38] Gonçalves S, Fernandez-Sanchez R, Sanchez-Niño MD, Tejedor A, Neria F, Egido J, et al. Tyrphostins as potential therapeutic agents for acute kidney injury. Curr Med Chem 2010;17:974–86.

[39] Balachandra S, Genovese T, Mazzon E, Di Paola R, Thiemerman C, Siriwardena AK, et al. Inhibition of tyrosine-kinase-mediated cellular signaling by tyrphostins AG 126 and AG556 modulates murine experimental acute pancreatitis. Surgery 2005;138:913–23.

[40] Genovese T, Mazzon E, Esposito E, Muià C, Di Paola R, Crisafulli C, et al. Inhibition of tyrosine kinase-mediated cellular signalling by Tyrphostins AG126 and AG556 modulates secondary damage in experimental spinal cord trauma. Neuropharmacology 2007;52:1454–71.

[41] Kim YJ, Lee CS. Tyrosine kinase inhibitor AG126 reduces 7-ketocholesterol-induced cell death by suppressing mitochondria-mediated apoptotic process. Neurochem Res 2010;35:603–12.